A&A 393, L11–L14 (2002)
DOI: 10.1051/0004-6361:20021126

Astronomy & Astrophysics

Spicule formation by ion-neutral damping

S. P. James and R. Erdélyi

Space and Atmosphere Research Center, Department of Applied Mathematics, University of Sheffield, The Hicks Building, Hounsfield Road, Sheffield S3 7RH, UK
e-mail: s.p.james@shef.ac.uk; e-mail: robertus@shef.ac.uk

Received 11 July 2002 / Accepted 2 August 2002

Abstract. The possible mechanism of generation of spicules by Alfvénic waves is studied in dissipative MHD where dissipation is mainly caused by ion-neutral collision damping, as suggested by Haerendel (1992).
Ion-neutral damping becomes non-negligible at the high cyclic frequencies involved, typically greater than 0.1 Hz, and the potential role played by this effect in both forming and supporting solar spicules is investigated.
The propagation of high frequency Alfvén waves on vertically open solar magnetic flux tubes is considered. The flux tubes are taken to be axisymmetric and initially untwisted with the field strength declining from 1600 G in the photosphere to 20 G in the corona. Their propagation is investigated by numerically solving a set of fully nonlinear, dissipative 1.5D MHD equations with the waves being generated by a continuous sinusoidal driver introduced into the equation of angular momentum in the low atmosphere of the Sun.
Spicule-like structures with heights of around 5000−6000 km were formed. The formation was found to be primarily caused by the impact of a series of slow shocks generated by the continuous interaction between the upward propagating driven wave train and the downward propagating train of waves created by reflection off the transition region. At the lower end of frequencies considered the heating due to ion-neutral damping was found to provide only a small benefit due to the increased thermal pressure gradient. At higher frequencies, whilst the heating effect becomes stronger, the much reduced wave amplitude reaching the transition region hinders spicule formation. The adiabatic results suggest that *ion-neutral damping may not support spicules* as described by Haerendel (1992). However, the effect is highly sensitive to the level of ionisation and therefore the energy balance. Including the effects of thermal conduction and radiation may well lead to different results and thus it would be premature to dismiss the mechanism at this point.

Key words. magnetohydrodynamics (MHD) – waves – Sun: transtition region – Sun: faculae, plages – Sun: atmosphere – Sun: chromosphere

1. Introduction

Solar spicules are long, thin cylindrical jet-like structures seen above the solar limb and best observed in strong chromospheric emission lines. They appear to be guided along the intense magnetic flux tubes at supergranule boundaries. Widths are 300−1500 km (Nishikawa 1988) which is similar to the spatial resolution of the observing instrumentation and, as a result, there is some disagreement on their properties in the literature. According to the general consensus (Beckers 1972; De Pontieu 1999; Sterling 2000) matter of approximately chromospheric densities (3×10^{-13} g cm^{-3}) and temperatures (5000−10 000 K) ascends with speeds of 25 km s^{-1} to heights of 5000−15 000 km above the photosphere. Typical lifetimes are 5−15 min after which the spicule is observed either to fall with velocity similar to the ascent velocity or occasionally to fade from view. Density and temperature are both fairly constant along the spicule length. Some spicules are believed to rotate rapidly. Ruždjak (1977) found that peripheral rotational velocities of 25 km s^{-1} gave theoretical line profiles similar to those observed.

It is unclear whether the spicule rise is ballistic or not (Nishikawa 1988). The high initial velocities of about 80 km s^{-1} required to produce spicules of sufficient height have not been observed on the disk although it should be noted that this may be a consequence of the low resolution. There is evidence of signal propagation speeds of up to 300 km s^{-1} (Hasan & Keil 1984). This is much larger than the local sound speed of around 20 km s^{-1} but similar to the local Alfvén speed, suggesting magnetic waves may play an important role in spicule formation.

Because the ascent and descent velocities of spicules are similar to the Alfvén and sound speeds of the upper chromosphere, any realistic investigation of their evolution must be

Send offprint requests to: R. Erdélyi,
e-mail: robertus@shef.ac.uk

non-linear. For this reason, most previous studies have taken the form of 1 D and 1.5 D numerical simulations, both hydrodynamic and magnetohydrodynamic. A number of potential formation mechanisms have been considered, an excellent overview of which may be found in Sterling (2000).

This work concentrates on ion-neutral damping of high frequency Alfvén waves as the driver for spicule formation, as originally proposed by Haerendel (1992). In the photosphere and chromosphere the solar plasma is only partially ionised. Changes in the magnetic and electric fields directly impact the ion fluid but the neutral fluid is indirectly affected, being collisionally coupled to the ions. At characteristic frequencies well below the neutral-ion collision frequency the slippage between the neutral and ion fluids is unimportant, but at sufficiently high frequencies Alfvén wave damping and dissipation can occur. Haerendel (1992) and De Pontieu & Haerendel (1998) showed that this effect produces a net waveperiod averaged force in the direction of wave propagation which, for realistic parameters of the solar atmosphere, can support a spicular structure against gravity. De Pontieu (1999) numerically investigated this effect by using an essentially 1D hydrodynamic model which incorporated the widening of a solar magnetic flux tube by looking at the evolution along a cylinder of flux lines and included the heating and coupling into vertical momentum due to wave damping by applying the WKB approximation to plane polarised small amplitude Alfvén waves. It was found that structures resembling solar spicules could indeed be generated and supported by this mechanism under these approximations, though for the parameters chosen, the heights of around 6000 km were toward the lower end of the typically quoted observational range. Whilst the WKB approximation was used in the linear limit, the velocities occurring in the simulation were in violation of this limit. It is therefore reasonable to believe that nonlinear effects may have a definite impact on the results. In addition, the WKB assumption breaks down in the transition region where the Alfvén speed increases by an order of magnitude in around 200 km. The intention here is to extend the model to 1.5 D fully dissipative and nonlinear MHD simulations, enabling investigation of the effects of nonlinearity, wave reflections off the transition region and more accurate consideration of the small scale structure of the results.

2. Details of the model

Consider a rigid, vertical, axisymmetric and initially untwisted flux tube. We define a local orthogonal curvilinear coordinate system by z, the distance along a field line, θ, the azimuthal angle about the axis of symmetry and ξ, a coordinate measured in the $\hat{\boldsymbol{z}} \times \hat{\boldsymbol{\theta}}$ direction. We assume $v_\xi = 0$ and $\partial/\partial\theta = 0$. The heating due to wave damping is included but otherwise the problem is considered adiabatic. The basic MHD equations yield:

$$\frac{\partial}{\partial t}\left(\frac{\rho}{B_z}\right) + \frac{\partial}{\partial z}\left(\frac{\rho v_z}{B_z}\right) = 0\,, \tag{1}$$

$$\frac{\partial}{\partial t}\left(\frac{\rho r v_\theta}{B_z}\right) + \frac{\partial}{\partial z}\left(\frac{\rho r v_\theta v_z}{B_\mathrm{s}}\right) = \frac{1}{\mu_0}\frac{\partial}{\partial z}(rB_\theta)\,, \tag{2}$$

$$\frac{\partial}{\partial t}\left(\frac{\rho v_z}{B_z}\right) + \frac{\partial}{\partial z}\left(\frac{\rho v_z^2}{B_z}\right) = -\frac{1}{B_z}\left[\frac{\partial p}{\partial z} + \rho g - \frac{v_\theta^2}{r}\frac{\partial r}{\partial z} + \frac{B_\theta}{\mu_0 r}\frac{\partial}{\partial z}(rB_\theta)\right], \tag{3}$$

$$\frac{\partial}{\partial t}\left(\frac{e}{B_z}\right) + \frac{\partial}{\partial z}\left(\frac{e v_z}{B_z}\right) = -p\frac{\partial}{\partial z}\left(\frac{v_z}{B_z}\right) + \frac{s}{B_z \mu_0^2 \sigma_0 r^2}\left[\frac{\partial}{\partial z}(rB_\theta)\right]^2, \tag{4}$$

$$\frac{\partial}{\partial t}\left(\frac{B_\theta}{rB_z}\right) + \frac{\partial}{\partial z}\left(\frac{B_\theta v_z}{rB_z}\right) = \frac{\partial}{\partial z}\left(\frac{v_\theta}{r}\right) + \frac{1}{\mu_0}\frac{\partial}{\partial z}\left(\frac{s}{B_z r^2 \sigma_0}\frac{\partial}{\partial z}(rB_\theta)\right), \tag{5}$$

where $e = \frac{p}{\gamma - 1} + n_\mathrm{e}\chi_\mathrm{H}$ is the internal energy, the sum of the thermal and ionisation energies, and s is the ion slip, a measure of the slippage between the ion and neutral fluids. Details of the method used in calculating the ionisation and ion slip can be found in De Pontieu (1996). The initial pressure and temperature profiles are taken from the VAL IIIc model atmosphere (Vernazza et al. 1981). The density profile is then calculated assuming a perfect gas law and initial hydrostatic equilibrium. The numerical grid is non-uniform with spatial resolution of at least 20 grid points per wavelength at all positions and times in the simulation. A flow-through boundary condition, $\partial/\partial z = 0$, is applied to all variables at both boundaries. The adiabatic constant is $\gamma = 5/3$. The B_z component of magnetic field is given by an analytic function as described by De Pontieu (1996), two parameters of which are the coronal and surface magnetic fields. In this work, the surface and coronal vertical magnetic field is taken to be 1600 G and 20 G respectively.

Alfvén waves are launched by the addition of a localized artificial body force in the equation of angular momentum,

$$F = A(z)\sin(\omega t), \tag{6}$$

centered at $z = 600$ km in height. This force could represent the perturbations at the footpoint of the flux tube caused by granular buffeting. The numerical solution is obtained using the Versatile Advection Code developed by Tóth (1996). Flux corrected transport schemes are used, chosen for their ability to accurately and stably handle the strong shocks which arise in the simulations.

3. Results

Figure 1 shows the evolution of the density profile with time for a wave period of 4 s and initial amplitude 20% of the background Alfvén speed. Figure 2 shows the velocity profile of the transition region, identified with the top of the structure and visible in Fig. 1 as the point at which the density becomes relatively constant. The wavefront reaches the transition region at about 50 s and starts to push it upwards. The plasma is then decelerated by gravity. There is a sharp increase in velocity with a period of about 20 s. Somewhat more than half of the Alfvén

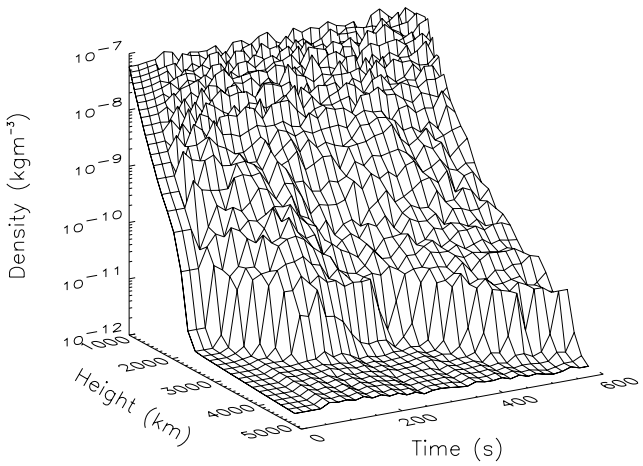

Fig. 1. Time evolution of the density profile for 4 s wave period, a characteristic high frequency, initial amplitude 20% and 20 G coronal magnetic field.

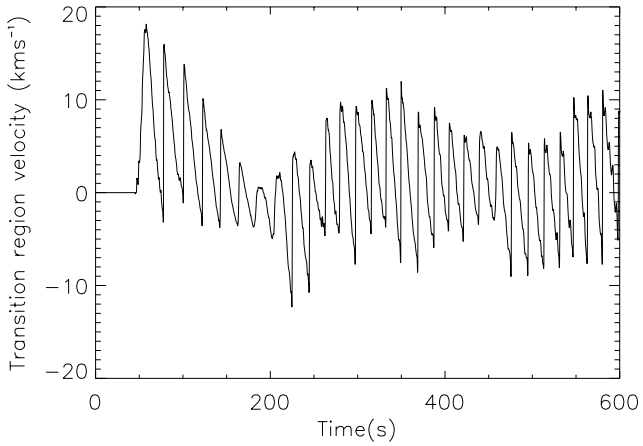

Fig. 2. Transition region velocity for the simulation in Fig. 1.

wave flux is reflected off the transition region resulting in a downward propagating train of reflected waves. This reflected wave train interacts with the upward propagating waves resulting in a series of shocks which propagate upward at the slow speed. The initial variation in shock strength, as measured by the increase in transition region velocity they cause, is unsurprising because the length of interaction which produces each subsequent shock increases as the reflected wave train propagates downwards. After around 100 s, the reflected wave train reaches the driving wave source. From this time on, the length of interaction for subsequent shocks is similar. Shocks formed after 100 s reach the transition region from around 200 s after which the shock strength becomes more uniform.

Figure 3 shows the motion of the transition region for three runs with identical parameters with the damping term in the induction equation and the heating term in the energy equation turned on or off as appropriate. The inclusion of damping alone makes little difference whilst the inclusion of heating increases the height of the structure. Evolution of the structure is *dominated by the shocks rather than the force from ion-neutral damping predicted by the linear WKB theory.* However,

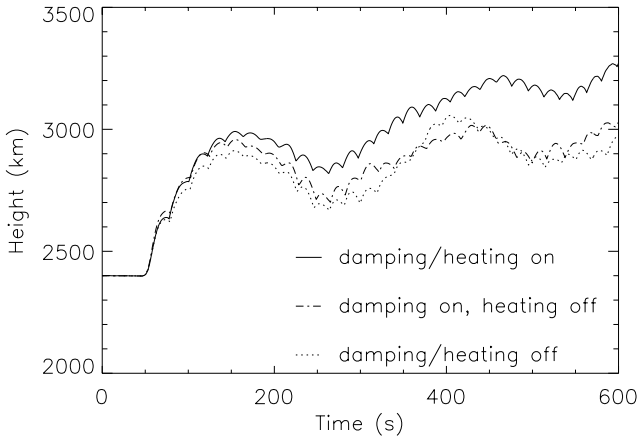

Fig. 3. Transition region position against time for 4 s wave period, 20% initial amplitude and 10 G coronal magnetic field with damping and heating neglected (dotted line), damping included but heating neglected (dash-dot line) and both damping and heating included (full line).

the heating from damping has a definite effect, increasing the thermal pressure gradient and helping to support the plasma against gravity, resulting in greater heights. At longer wave periods, the three results converge as the damping and resultant heating become negligible. At shorter wave periods, the waves become too strongly damped in the upper chromosphere and the reduction in wave amplitude reaching the transition region overcomes the positive benefit from increased heating resulting in smaller structures.

The variation of transition region height by wave period is shown in Fig. 4. There is a clear trend of increasing height with increasing time period. The initial velocities are largely determined by the amplitude of the wavefront. At 2 s time period, the damping is significant and the much reduced wave amplitudes reaching the transition region account for the much reduced initial velocity. At the longer wave periods, damping has a reduced effect and the initial velocities are more similar.

A study of the reflection of Alfvén waves off the transition region in our model shows that longer period waves are more strongly reflected. The increased strength of the reflected wave train leads to stronger shocks forming which would help to explain the increased velocities and heights. Countering this, the heating effect will decrease with increasing time period, reducing the ability of the thermal pressure gradient force to support the structure against gravity. This helps to explain why the 4 s and 6 s results show a more gradual increase in height after the initial rise as continuous heating makes more of a contribution relative to the impact of the slow shocks.

Figure 5 shows the temperature and density profiles at the end of one characteristic simulation with the initial profiles shown for reference. The heating is clearly in evidence with the choromospheric material having been heated to between 10 000 K and 15 000 K. The density profile shows the stratification into high and low density regions caused by the interaction of the upward propagating and reflected wave trains. The profiles are similar in character for all parameters so far considered. The level of heating reduces with increasing

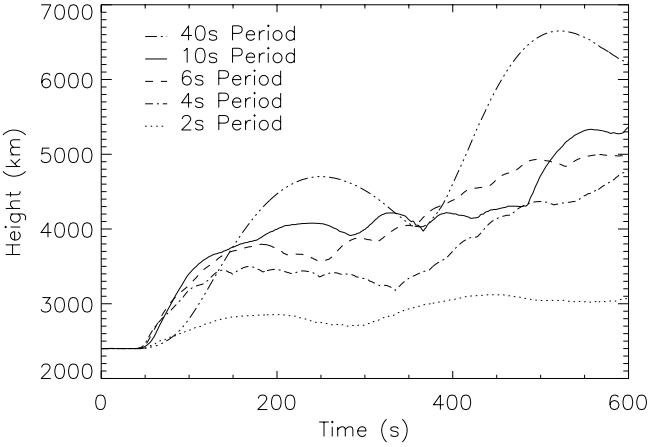

Fig. 4. Transition region position against time for initial amplitude 20% and a coronal magnetic field of 20 G. The results of five different runs with periods ranging between 2 s and 40 s are shown.

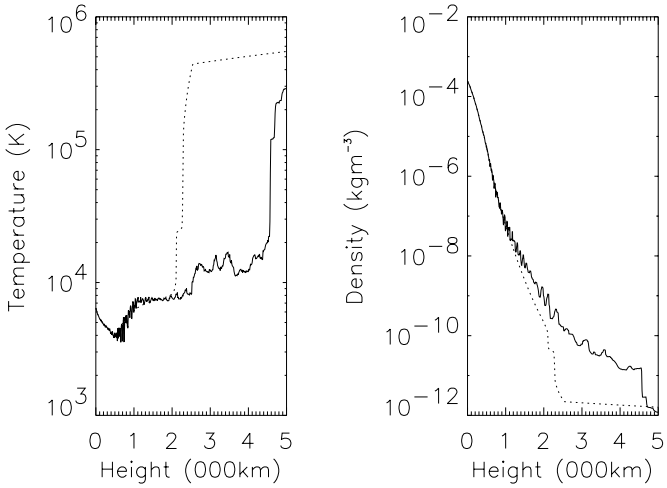

Fig. 5. Temperature and density profiles for the case with 4 s period, 20% initial amplitude and 20 G coronal magnetic field. The full lines shows the profiles at 600 s whilst the dotted lines show the initial profiles for comparison.

wave period but the peaks and troughs in both the density and temperature profiles become considerably more pronounced, reaching as much as a factor of 10 apart for 10 s wave periods. Such fine structure may not be visible in observations so that the results are not necessarily in contradiction with the fairly flat profiles observed. The inclusion of thermal conduction would probably reduce the fine structure in the temperature profile.

4. Conclusion

1.5 D dissipative and fully nonlinear MHD numerical simulations were run to test Haerendel's (1992) hypothesis that ion-neutral damping of Alfvén waves, which becomes important in the solar atmosphere for cyclic frequencies greater than approx. 0.1 Hz, can provide a mechanism for the formation and support of solar spicules. Waves were launched by a continuous localised source in the photosphere. The initial impact of the wavefront was found to push the transition region upward. The subsequent evolution of the structure was found to be dominated by the slow shocks formed by the continuous interaction between the upward propagating wave train and the waves reflected off the moving transition region. The structures formed had density and temperature profiles broadly in agreement with observations but heights and velocities were slightly below those observed. Increasing the initial wave amplitude parameter should help to produce greater heights and velocities and will be the subject of future work.

Alfvén wave damping helped to heat the structure but the coupling into vertical momentum predicted by the WKB linear analysis was only a minor effect in the subsequent evolution. Since the effect depends on the presence of neutrals in the plasma, inclusion of thermal conduction and radiative losses may increase its importance by lowering the temperature and increasing the neutral density. As well as the WKB approximation initially being violated in the transition region, it is also violated everywhere once the interaction of upward propagating and reflected waves results in stratification into high and low density regions. It is perhaps not surprising then that the anticipated effects failed to materialise. This stratification is primarily the result of a partially standing wave. A more random source of Alfvénic disturbances should reduce this effect and will also be studied in future work. In particular, a driver containing both low and high frequency components may overcome the insufficient temperatures obtained by most rebound shock models with low frequency drivers.

Acknowledgements. This work was supported by Particle Physics and Astronomy Research Council (PPARC) grant PPa/S/S/2000/02983. The authors thank B. De Pontieu for the many discussions and comments. RE acknowledges M. Kéray for patient encouragement and the financial support obtained from the NSF, Hungary (OTKA, Ref. No. TO32462) and The Nuffield Foundation (NAL/99-00).

References

Beckers, J. M. 1972, ARA&A, 10, 73
De Pontieu, B. 1996, Ph.D. Thesis, University of Ghent, Belgium
De Pontieu, B. 1999, A&A, 347, 696
De Pontieu, B., & Haerendel, G. 1998, A&A, 338, 729
Haerendel, G. 1992, Nature, 360, 241
Hasan, S. S., & Keil, S. L. 1984, ApJ, 283, 75
Nishikawa, T. 1988, Publ. Astron. Soc. Jpn, 40, 13
Ruždjak, V. 1977, Bull. Astron. Inst. Czech., 28, 198
Sterling, A. C. 2000, Sol. Phys., 196, 79
Tóth, G. 1996, Astrophys. Lett. Commun., 34, 245
Vernazza, J. E., Avrett, E. H., & Loeser, R. 1981, ApJ, 45, 635